metals

MDPI

Article

Effect of Severe Plastic Deformation on the Conductivity and Strength of Copper-Clad Aluminium Conductors

Rimma Lapovok [1,2,*], Michael Dubrovsky [1], Anna Kosinova [1] and Georgy Raab [3]

1. Department of Materials Science and Engineering, Technion-Israel Institute of Technology, Haifa 3200003, Israel
2. Institute for Frontier Materials, Deakin University, Waurn Ponds, Victoria 3216, Australia
3. Institute of Physics of Advanced Materials, Ufa State Aviation Technical University, Ufa 450000, Russia

* Correspondence: r.lapovok@deakin.edu.au; Tel.: +61-419897830

Received: 4 August 2019; Accepted: 27 August 2019; Published: 1 September 2019

check for updates

Abstract: Aluminium rods with different copper sheath thicknesses were processed by severe plastic deformation at room temperature and then annealed, to join the constituent metals and produce a nanocrystalline microstructure. A study of the effects of the deformation parameters, copper cladding thickness and annealing temperature on the electrical conductivity and hardness of the conductors is reported. It is shown that an interface forms between constituents because of intermixing in the course of severe shear deformation under high hydrostatic pressure and diffusion during the subsequent annealing. The effective conductivity of the aluminium copper-clad conductor dropped after deformation, but was recovered during annealing, especially during short annealing at 200 °C, to a level exceeding the theoretically predicted one. In addition, the annealing resulted in increased hardness at the interface and copper sheath.

Keywords: aluminium copper-clad rod; hardness; effective electrical conductivity; severe plastic deformation

1. Introduction

Copper-clad aluminium (CCA) wire is a well-known conductor produced by extrusion of an aluminium rod in a copper can. Al-Cu hybrid materials combine the high conductivity of copper with the lightweight of aluminium. These wires, used in high frequency applications, offer the advantages of better conductivity due to the skin effect, and higher strength and corrosion resistance compared to all-aluminium wire, while costing less than all-copper wire [1]. The well-known study of copper-clad wires [2] shows that at very high frequencies, these wires' electrical properties approach those of a solid copper conductor.

Extrusion of aluminium–copper bi-metallic rods is performed in several reduction steps that are combined with annealing to restore the materials' ductility. The annealing; however, leads to enhanced diffusion between constituents and the formation of brittle aluminium–copper intermetallic compounds at the interface [3,4], which affects the composite wire's conductivity [5,6]. The interface formed between aluminium and copper consists of a number of intermetallic compounds (up to 13 stable intermetallic phases according to Murray [7]), the formation of which depends on the annealing temperature and duration. The conductivity of these phases is shown to be many times lower than that of the constituent materials [5,6].

A different approach, considered here, suggests replacing the extrusion process with a severe plastic deformation (SPD) process [8,9]. We have already used a similar method for aluminium–steel conductors in [10]. Since SPD introduces a gigantic shear strain into the processed material, especially in the vicinity of the interface [11,12], it is expected that the bonding between aluminium and copper will appear at low temperatures due to intermixing. During SPD processing, this brittle intermetallic layer will either not form or be destroyed and dissolved, which would improve the strength and conductivity of the resulting wire. Low-temperature annealing was applied to assist the diffusion and strengthening of the bond region.

In this work, aluminium rods with different copper sheath thicknesses were processed using SDP at room temperature and then annealed. A study of the effect of SPD parameters, copper cladding thickness, and annealing temperature on the electrical conductivity and strength of CCA conductors is reported below.

2. Material and Experimental Techniques

Commercially-pure Al 1050 rods (Fe content of 0.352 ± 0.015 wt%) were inserted into 99.9% pure copper tubes with an outer diameter of 10 mm and wall thicknesses of 0.4 and 0.7 mm, in such a manner that compression was exercised on the aluminium rod surface, Figure 1. The copper tube was heated to 150 °C to extend its diameter sufficiently to insert the cold aluminium rod. After the tube cooled down, it shrank and created the compressive stresses at the surface of the rod. The initial average grain sizes of the aluminium and copper were around 58 ± 25 μm and 96 ± 37 μm, respectively.

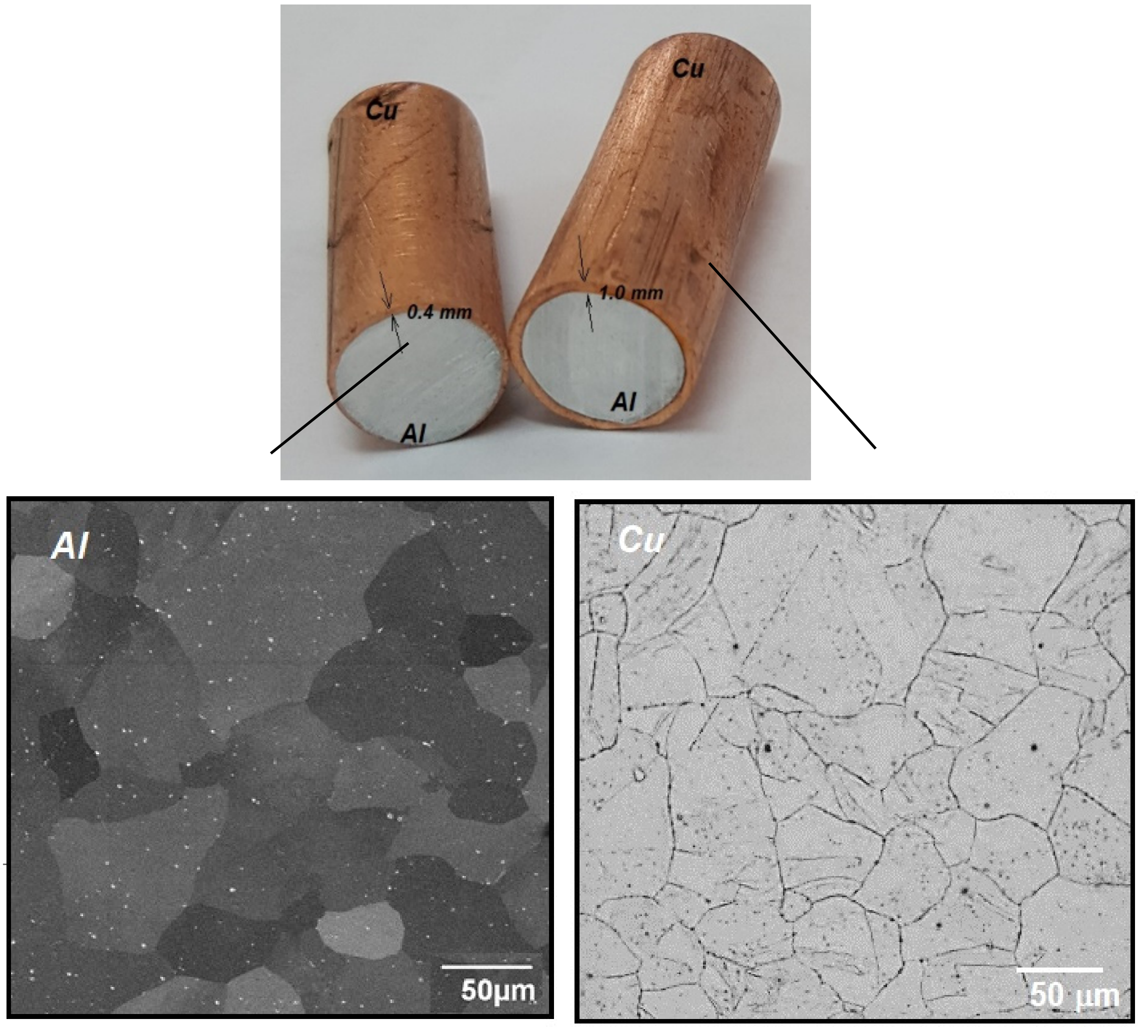

Figure 1. Aluminium rods cladded by copper with different thicknesses before deformation. (The left image is a backscattered SEM image and the right one is an optical microscope image.).

Samples were subjected to one and two passes of equal channel angular pressing (ECAP) using Route A (no rotation between passes) and Route B_C (90° rotation between passes). This was followed by annealing according to two different schedules—namely, 200 °C for 5 min and 120 °C for 2 h.

The alloy's microstructure in all conditions was characterised by high resolution scanning electron microscope (HRSEM) Zeiss Ultra Plus, Jena, Germany). The interface zone, which was formed by intermixing and diffusion, was characterised by energy-dispersive X-ray spectroscopy (EDX) (Oxford Instruments, UK) in HRSEM.

A Vickers hardness test was performed using a Buehler MMT-7 micro-hardness tester (Lake Bluff, IL, USA). The samples were polished with 500 grit sandpaper and 10 hardness measurements were performed for each sample using a load of 200 g. The standard deviations from the mean value were calculated as between 2.8 and 3.6.

The electrical resistivity of all these samples was measured at room temperature using the four-point constant-current (DC) method. The resistivity was calculated as:

$$\rho = \frac{V}{I} \cdot \frac{S}{l'}, \tag{1}$$

where V is the voltage change between two points on the side of the tubular samples at a distance of l' = 5 mm from each other, measured by a Keithley 2700 multi-meter. In addition, I = 10 A was the constant current applied by a TDK Lambda current source through the top and bottom sides of the samples over an area S of the tube cross-section, which was in contact with copper plates under ~250 Pa pressure.

3. Results and Discussion

3.1. The Grain Refinement during SPD and Annealing

Extreme grain refinement was observed in the deformed hybrid samples, especially in the outer copper cladding where friction added to the severity of the shear strain. The microstructure, after two ECAP passes (Route B_C), followed by annealing, is shown in Figure 2. Due to SPD, the grain size in the aluminium rod was reduced to 410 ± 150 nm and in the copper sheath to 180 ± 90 nm. The annealing did not cause any grain growth in the copper as the temperature–time schedules were chosen to be within the region of thermal stability suggested for high purity copper in [13]. The presence of Fe precipitates decorating the grain boundaries in the aluminium also prevented grain growth in the aluminium rod. Therefore, the annealing resulted in recovery of the dislocations within the ultrafine grains of both constituents of the hybrid material and formation of a clean (free of dislocation within the grain interior) ultrafine microstructure with sharp boundaries.

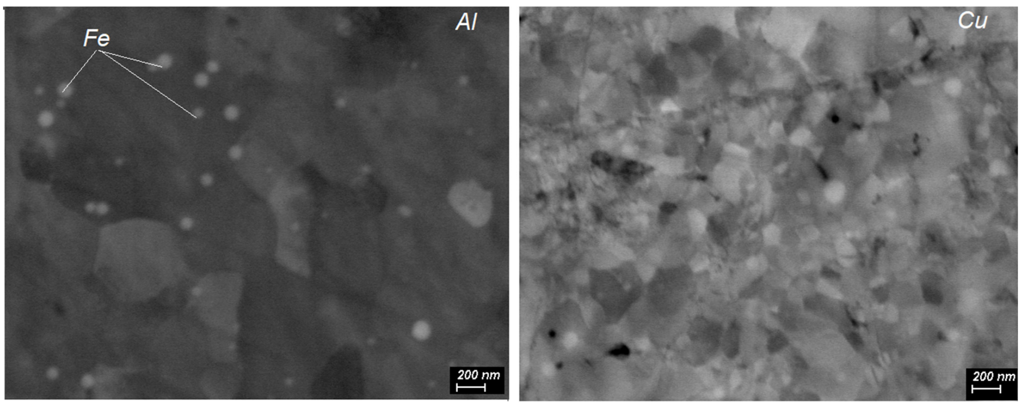

(**a**) (**b**)

Figure 2. SEM images (back-scattered electrons) of the microstructure after two ECAP passes (Route B_C) and annealing. (**a**) Aluminium core; (**b**) copper sheath.

3.2. Interface Formation during Room Temperature Deformation

Interface formation is typically governed by three mechanisms, namely, intermixing, inter-diffusion and phase formation [14,15]. Room temperature deformation leads to intermixing when the surface asperities are crushed during contact under high hydrostatic pressure and severe shear deformation [14], mixing the constituents in a swirl flow (Figure 3). As a result of SPD; however, grain refinement by rearrangement of accumulated dislocations takes place and many new defects are introduced (for example, solid solutions of constituent atoms).

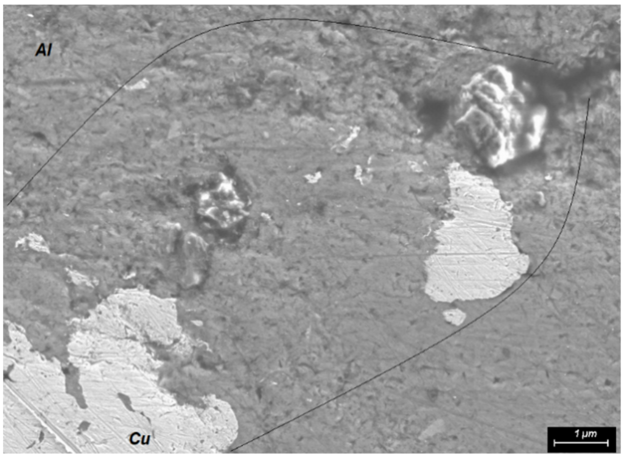

Figure 3. The inter-mixing zone resulting from intensive shear of constituents under high hydrostatic pressure (black lines show the boundary of the intermixing zone where random islands of copper within the aluminium can be seen).

Subsequent static annealing results in accelerated inter-diffusion, which adds to the formation of the interface, Figure 4. SEM-EDX analysis of selected points in the vicinity of interface points 1–5 shows the diffusion of copper atoms into the aluminium matrix to a depth of about 750 nm while aluminium atoms diffused into the copper matrix to a depth of around 250 nm, Figure 4a. The concentration of aluminium at a distance of ~200 nm from the interface within the copper matrix is around 12 at%, Figure 4b, which is below the concentration required to form any intermetallic compound [7]. These results are similar to previously reported observations of interface formation in aluminium/copper bimetallic tubes made by high-pressure tube shearing [11], and the formation of intermetallic compounds detrimental to conductivity was not observed.

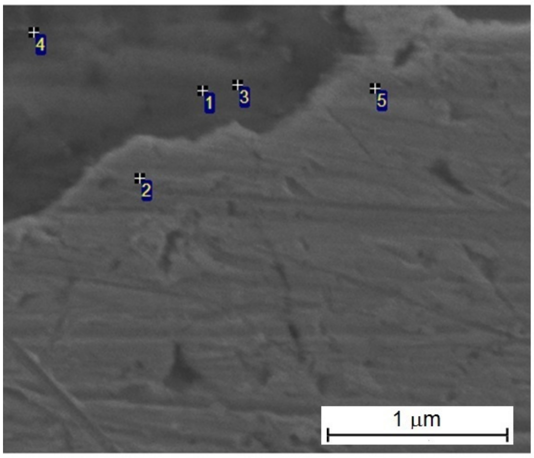

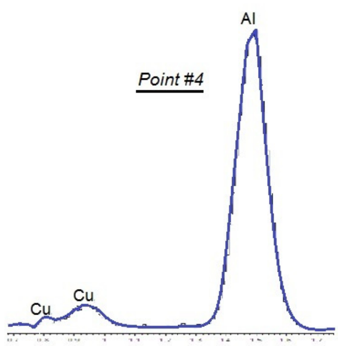

Element	#1	#2	#3	#4	#5
Al, at%	98.67	0.82	99.11	97.36	0.52
Cu, at%	1.33	99.18	0.89	2.64	99.48

(**a**)

Figure 4. *Cont.*

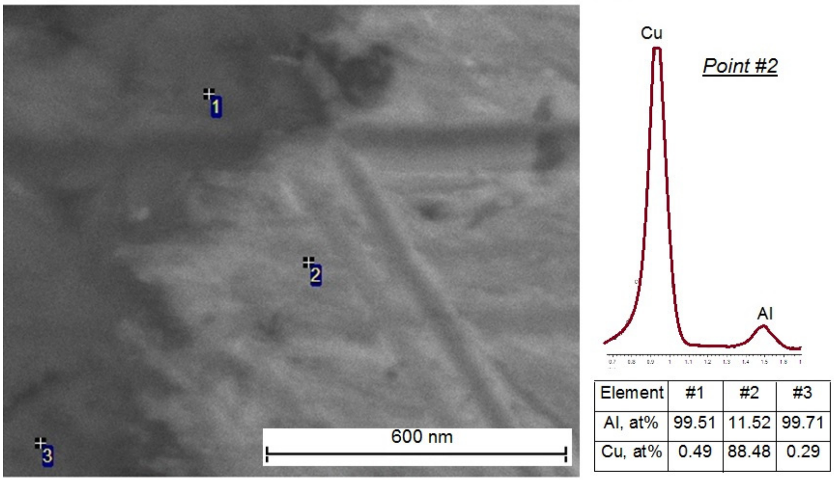

Element	#1	#2	#3
Al, at%	99.51	11.52	99.71
Cu, at%	0.49	88.48	0.29

(**b**)

Figure 4. SEM-EDX analysis of selected points in the vicinity of the interface at two locations: (**a**) and (**b**).

3.3. Hardness

It can be seen, Figure 5, that the aluminium hardness raises gradually as the number of passes increases. Due to the small number of ECAP passes; however, this increase is insignificant, from ~36 HV at the initial annealed conditions to 40–42 HV after one ECAP pass and to 45–48 HV after two ECAP passes. In contrast, the copper cladding hardness rises significantly from its initial annealed value of 58 HV to 85–105 HV after deformation. The Cu-Al interface hardness displays a gradual increase compared to the aluminium hardness due to non-homogeneous intermixing of constituents.

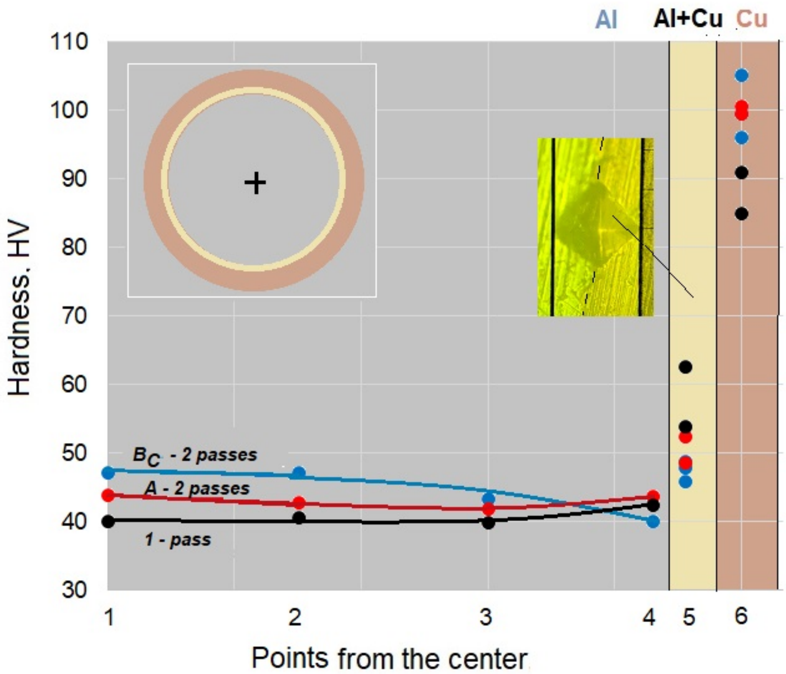

Figure 5. Hardness after deformation versus distance from the centre measured at six points in the aluminium part (points 1–4), at the interface (point 5) and in the copper cladding (point 6). (The two similarly coloured points at the interface and at the copper cladding represent measurements for thick and thin sheaths).

It should be noted that annealing results in a decrease in the aluminium hardness and an increase in the interface and copper sheath hardness (Figure 6). The effect of increased strength in ultrafine-grained (UFG) materials due to annealing has been observed and discussed quite recently in several publications [16,17]. The reason for this phenomenon was believed to be the segregated impurities at the grain boundaries. Nevertheless, the issue has still not been elucidated as high purity metals in a nano-crystalline state demonstrated a similar effect. Further, several UFG materials show hardening by annealing while others do not. For example, copper annealed after high-pressure torsion at temperatures in the range of 0.25 to 0.3 Tm (depending on the copper purity) demonstrated similar hardening behaviour, which was explained by agglomeration and annihilation of deformation-induced vacancies [18].

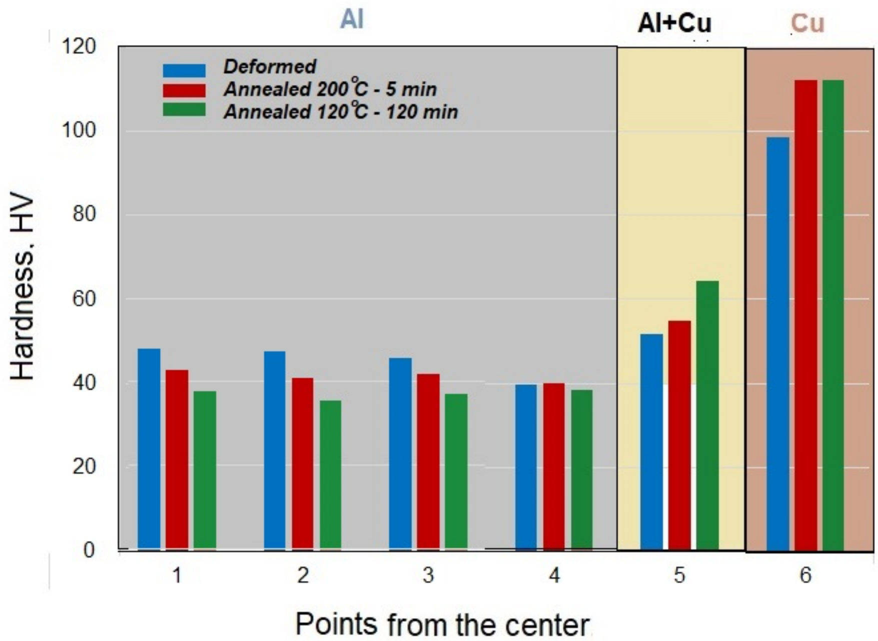

Figure 6. Comparison of hardness after deformation (two passes Route B_C) and annealing measured at six points located in the aluminium part (points 1–4); at the interface (point 5); and in the copper part (point 6) (measured for sample with thick sheath).

In our case, the temperature of annealing was chosen within the range defined for copper in [17]. Subsequently, hardening of the copper and the interface zone was observed. The chosen temperature; however, was high enough to change the crystallite size and dislocation density in aluminium, causing softening of the aluminium core.

3.4. Electrical Conductivity

The electrical conductivity for parallel connection of conductors can be calculated using the rule of mixture:

$$\sigma_{ef} = \sigma_{Al} f_{Al} + \sigma_{Cu} f_{Cu} = \sigma_{Al}(1 - f_{Cu}) + \sigma_{Cu} f_{Cu}$$

The effective conductivity of aluminium–copper-clad conductors, calculated using theoretical conductivities for aluminium and copper constituents, is represented by the dashed line in Figure 7. In reality; however, the effective conductivity was about 10% lower than the ideal theoretical value, and was in the range of 55% to 60% IACS. The low initial conductivity could be explained by the Fe high content in the solid solution and is in line with results published in [18].

The electrical conductivity measured after deformation shows strong dependence on the severity of the deformation. The conductivity after one pass dropped from the initial value to 36.1% ± 3.6% IACS for a thin sheath and to 60.5% ± 2.4% IACS for a thick sheath. The conductivity decreased further after two deformation passes, more when using Route B_C than when using Route A.

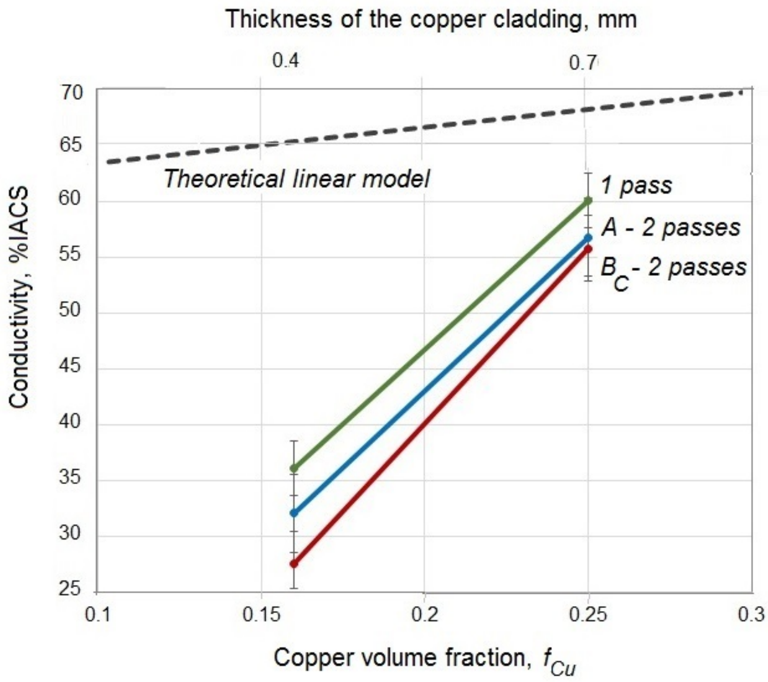

Figure 7. Effective conductivity versus thickness of copper cladding after deformation.

Short annealing at 200 °C restored conductivity to a greater extent than prolonged annealing at 120 °C, especially for samples deformed by one or two passes along Route B_C, as seen in Figure 8. It should be noted that conductivity after annealing of samples with the thick sheath exceeded the theoretical values (~68%IACS), represented by the dashed line in Figure 7 and reached ~75% IACS. Connectivity of samples with thin sheath was worse due to defects introduced by SPD and leads to the conclusion that the cladding thickness has the lower limit on the benefits offered by this cladding technique.

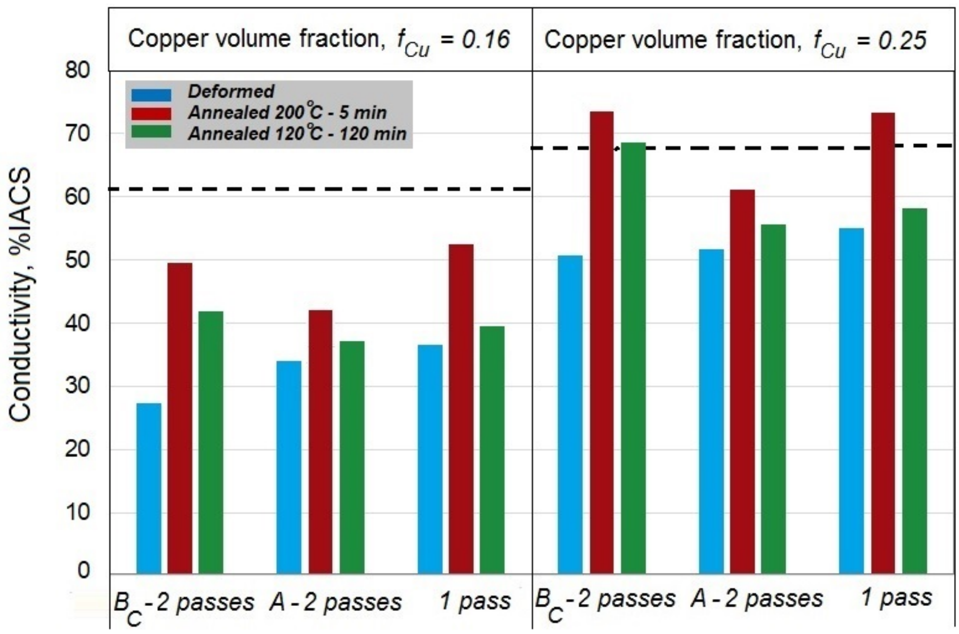

Figure 8. Effective conductivity after deformation and two annealing schedules for different thicknesses of copper cladding (the dashed line shows the theoretically predicted level of conductivity).

4. Conclusions

Copper-clad aluminium rods with different copper sheath thicknesses were produced by SPD at room temperature, followed by annealing rather than by conventional extrusion at elevated temperatures. Detrimental formation of intermetallic phases with low conductivity was not observed. An interface between constituents formed by their severe intermixing due to large shear, high hydrostatic pressure and possibly diffusion during annealing.

Severe plastic deformation was performed using ECAP for one or two passes along Routes A and B_C. Extreme grain refinement down to the nano-range size as a result of SPD processing was shown. The UFG microstructure remained stable during annealing. It is demonstrated that to achieve an interface without defects, ECAP must be performed on copper-clad aluminium rods with thickness of copper cladding at least 0.7 mm or higher.

The effective conductivity of aluminium copper-clad conductors dropped after deformation in proportion to the number of ECAP passes (more when using Route B_C than A). Annealing, especially short annealing at 200 °C; however, resulted not only in recovery of conductivity but in conductivity values exceeding the theoretically predicted ideal ones.

In addition, annealing resulted in an increase of hardness at the interface and in the copper sheath, which confirms the possibility of hardening UFG metals by annealing at temperatures in the range of 0.25 to 0.3 Tm. Thus, SPD and short annealing at the temperature within this range could be used to produce lightweight conductors with high conductivity and strength.

Author Contributions: R.L.—conceptualization, funding acquisition, supervision, writing—original draft, analysis of results; M.D.—properties measurements; A.K.—microstructure characterization, analysis of results, writing—review & editing; G.R.—samples preparation and processing, analysis of results.

Funding: This research was funded by the EU Framework Program for Research and Innovation 'HORIZON 2020' (Grant-742098).

Acknowledgments: R. Lapovok acknowledges the Marie Curie Fellowship within the EU Framework Program for Research and Innovation 'HORIZON 2020'.

Conflicts of Interest: The authors declare no conflicts of interest.

References

1. Read, D. Copper Clad Aluminum in Electrical Application. *SAE Trans.* **1968**, *77*, 1920–1931. [CrossRef]
2. Miller, J.M. *Effective Resistance and Inductance of Iron and Bimetallic Wires*; Classic Reprint Series; Forgotten Books Publisher: London, UK, 2019; p. 76.
3. Hug, E.; Bellido, N. Brittleness study of intermetallic (Cu, Al) layers in copper-clad aluminium thin wires. *Mater. Sci. Eng. A* **2011**, *528*, 7103–7106. [CrossRef]
4. Braunovic, M.; Rodrigue, L.; Gagnon, D. Nanoindentation Study of Intermetallic Phases in Al-Cu Bimetallic System. In Proceedings of the 2008 IEEE 54th Holm Conference on Electrical Contacts, Orlando, FL, USA, 27–29 October 2008. [CrossRef]
5. Pfeifer, S.; Großmann, S.; Freudenberger, R.; Willing, H.; Kappl, H. Characterization of Intermetallic Compounds in Al-Cu-Bimetallic Interfaces. In Proceedings of the 2012 IEEE 58th Holm Conference on Electrical Contacts, Portland, OR, USA, 23–26 September 2012. [CrossRef]
6. D'Heurle, F.; Alliota, C.; Angilello, J.; Brusic, V.; Dempsey, J.; Irmischer, D. The deposition by evaporation of Cu-Al alloy films. *Vacuum* **1997**, *27*, 321–327. [CrossRef]
7. Murray, J.L. The Aluminium-Copper System. *Int. Met. Rev.* **1985**, *30*, 211–233. [CrossRef]
8. Valiev, R.Z.; Estrin, Y.; Horita, Z.; Langdon, T.G.; Zehetbauer, M.J.; Zhu, Y.T. Producing bulk ultrafine-grained materials by severe plastic deformation. *JOM* **2006**, *58*, 33–39. [CrossRef]
9. Valiev, R.Z.; Estrin, Y.; Horita, Z.; Langdon, T.G.; Zehetbauer, M.J.; Zhu, Y.T. Producing Bulk Ultrafine-Grained Materials by Severe Plastic Deformation: Ten Years Later. *JOM* **2016**, *68*, 1216–1226. [CrossRef]
10. Qi, Y.; Lapovok, R.; Estrin, Y. Microstructure and electrical conductivity of aluminium/steel bimetallic rods processed by severe plastic deformation. *J. Mater. Sci.* **2016**, *51*, 6860–6875. [CrossRef]

11. Lapovok, R.; Ng, H.P.; Thomus, D.; Estrin, Y. Bimetallic Copper-Aluminium Tube by Severe Plastic Deformation. *Scr. Mater.* **2012**, *66*, 1081–1084. [CrossRef]
12. Lapovok, R.; Qi, Y.; Ng, H.P.; Toth, L.S.; Estrin, Y. Gradient structures in thin-walled metallic tubes produced by continuous high pressure tube shearing process. *Adv. Eng. Mater.* **2017**, *19*, 1700345. [CrossRef]
13. Wang, Y.L.; Lapovok, R.; Wang, J.T.; Qi, Y.S.; Estrin, Y. Thermal behavior of copper processed by ECAP with and without back pressure. *Mater. Sci. Eng. A* **2015**, *628*, 21–29. [CrossRef]
14. Medvedev, A.E.; Lapovok, R.; Koch, E.; Höppel, H.W.; Göken, M. Optimisation of Interface Formation by Shear Inclination: Example of Aluminium-Cooper Hybrid Produced by ECAP with Back-Pressure. *Mater. Des.* **2018**, *146*, 142–151. [CrossRef]
15. Mendes, A.; Timokhina, I.; Molotnikov, A.; Hodgson, P.; Lapovok, R. Role of Shear in Interface Formation of Aluminium-Steel Multilayered Composite Sheets. *Mater. Sci. Eng. A* **2017**, *705*, 142–152. [CrossRef]
16. Renk, O.; Hohenwarter, A.; Schuh, B.; Li, J.H.; Pippan, R. Hardening by annealing: Insights from different alloys. In Proceedings of the 36th Risø International Symposium on Materials Science, Risø, Denmark, 7–11 September 2015; IOP Publishing: Bristol, UK, 2015; Volume 89. [CrossRef]
17. Cengeri, P.; Kerber, M.B.; Schafler, E.; Zehetbauer, M.J.; Setman, D. Strengthening during heat treatment of HPT processed copper and nickel. *Mater. Sci. Eng. A* **2019**, *742*, 124–131. [CrossRef]
18. Medvedev, A.; Murashkin, M.; Enikeev, N.; Valiev, R.Z.; Hodgson, P.D.; Lapovok, R. Optimization of strength-electrical conductivity properties in Al-2Fe alloy by severe plastic deformation and heat treatment. *Adv. Eng. Mater.* **2018**, *20*, 1700867. [CrossRef]